

Complex decoherence-free interactions between giant atoms

Lei Du,^{1,2} Lingzhen Guo,^{3,4} and Yong Li^{1,5}

¹*Center for Theoretical Physics and School of Science, Hainan University, Haikou 570228, China*

²*Center for Quantum Sciences and School of Physics,
Northeast Normal University, Changchun 130024, China*

³*Department of Applied Physics, Nanjing University of Science and Technology, Nanjing 210094, China*

⁴*Max Planck Institute for the Science of Light, 91058, Erlangen, Germany*

⁵*Synergetic Innovation Center for Quantum Effects and Applications,
Hunan Normal University, Changsha 410081, China*

(Dated: November 2, 2022)

Giant atoms provide a promising platform for engineering decoherence-free interactions which is a major task in modern quantum technologies. Here we study systematically how to implement complex decoherence-free interactions among giant atoms resorting to periodic coupling modulations and suitable arrangements of coupling points. We demonstrate that the phase of the modulation, which is tunable in experiments, can be encoded into the decoherence-free interactions, and thus enables the Aharonov-Bohm effect of photons when the giant atoms constitute an effective closed loop. In particular, we consider the influence of non-Markovian retardation effect arising from large separations of the coupling points and study its dependence on the modulation parameters.

I. INTRODUCTION

Giant atoms [1] nowadays become a powerful quantum optical paradigm, which breaks up a longstanding wisdom that atoms are usually modeled as single points based on the electric-dipole approximation. Specifically, giant atoms can be understood as quantum emitters that are coupled to a (propagating) bosonic field at multiple separate points. As the separation distances between different coupling points are comparable to the wavelength of bosonic field, giant atoms feature a peculiar self-interference effect leading to a series of unprecedented quantum optical phenomena, including frequency-dependent Lamb shift and relaxation rate [2, 3], unconventional bound states [4–11], advanced single-photon scatterings [12–19], non-Markovian decay dynamics [20–23], and chiral light-matter interactions [24–26], to name a few. Even more strikingly, by engineering the geometrical arrangements of the coupling points, a set of giant atoms can be made fully dissipationless but featuring field-mediated coherent interactions [27–29]. This phenomenon realizes the so-called decoherence-free interaction (DFI) that has potential important applications in quantum technologies, e.g., engineering large-scale quantum networks. Although DFIs can also be realized in discrete photonic lattices by tuning the atomic frequencies within the photonic band gaps [30–32], this kind of interactions, however, is typically of short range and only operates within certain bandwidths since they are mediated by overlapped atom-field bound states.

It is known that electrons can acquire path-dependent phases when traveling in a magnetic field [33], while photons/phonons are immune to physical magnetic fields due to their charge neutrality. Given this fact, many efforts have been made to create synthetic magnetic fields for bosonic systems [34–44]. While most of these seminal works have concentrated on systems where the targets

(e.g., atoms and resonators) are spatially close and non-Markovian retardation effects are typically ignored, very little is known about the effect of synthetic magnetic fields in large-scale quantum networks featuring field-mediated long-range interactions. Moreover, it is natural to ask if the DFIs between giant atoms, which are the result of a virtual-photon process, can be endowed with synthetic magnetism.

In this paper, we demonstrate how to realize complex DFIs between *detuned* giant atoms. By modulating the atom-field couplings (or the atomic transition frequencies) properly, the phase of the modulation can be encoded into the DFI. Such a complex DFI is tunable *in situ* and leads to the photonic Aharonov-Bohm effect when the effective Hamiltonian of the giant atoms has a closed-loop form. We find that the non-Markovian retardation effect, which is intrinsic to giant-atom systems, only introduces finite dissipation to the atoms without affecting their dynamics qualitatively. This detrimental effect can be mitigated with a smaller modulation frequency, yet an extremely slow modulation can smear the effect of synthetic magnetic field due to the contribution of anti-rotating-wave terms.

II. MODEL AND EQUATIONS

We start by considering two two-level giant atoms (labeled as atoms *A* and *B*, respectively), each of which is coupled to the one-dimensional waveguide at two coupling points. As shown in Fig. 1(a), the atom-waveguide coupling points are arranged in a braided manner which allows for a DFI between the two atoms [27, 28]: under certain conditions, both atoms do not dissipate into the waveguide yet there is a field-mediated coherent coupling between them. For simplicity, we assume that the coupling points are equally spaced by distance *d* (DFIs are allowed even if the coupling points are not equally spaced).

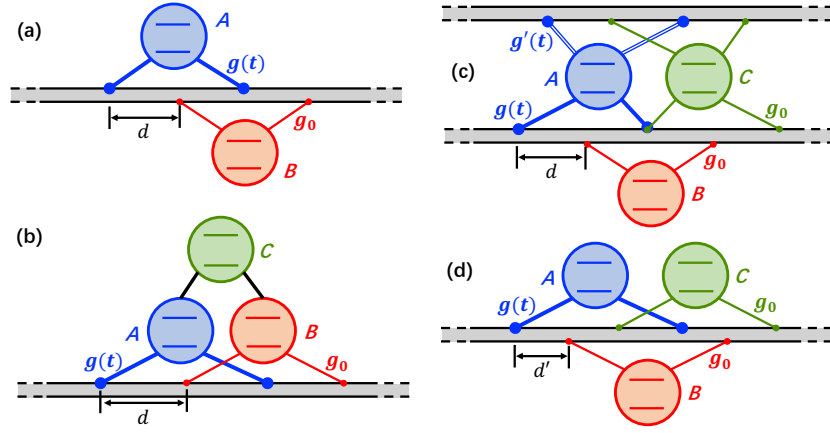


FIG. 1. Schematics of model architectures. (a) Two-level giant atoms A and B are coupled to each other via a time-dependent decoherence-free interaction. (b) A third atom C is coupled directly to A and B to form a closed-loop atomic trimer. (c) and (d) Protected all-to-all couplings for atoms A , B , and C resorting to (c) two different waveguides and (d) a single waveguide. Atoms B and C are assumed to be resonant with each other and detuned from atom A . The coupling points are equally spaced in all panels.

In contrast to the previous standard model where the atom-waveguide coupling strengths are constant [27, 28], here we assume that the coupling strength $g(t)$ of atom A is time-dependent and g_0 of atom B is constant (for each atom the coupling strength is assumed to be real and identical at the two coupling points). Moreover, we assume that there is a small detuning Δ between the transition frequencies of the two atoms. This detuning is crucial for realizing the synthetic magnetic field as will be shown below. In this case, the Hamiltonian of the model can be written as ($\hbar = 1$)

$$H = H_a + H_w + H_{\text{int}}, \quad (1)$$

$$H_a = \omega_0 \sigma_A^+ \sigma_A^- + (\omega_0 + \Delta) \sigma_B^+ \sigma_B^-, \quad (2)$$

$$H_w = \int dk \omega_k a_k^\dagger a_k, \quad (3)$$

$$H_{\text{int}} = \int dk [g(t) (1 + e^{2ikd}) \sigma_A^+ a_k + g_0 (e^{ikd} + e^{3ikd}) \sigma_B^+ a_k + \text{H.c.}], \quad (4)$$

where ω_0 is the transition frequency of atom A ; σ_A^+ and σ_B^+ (σ_A^- and σ_B^-) are the raising (lowering) operators of atoms A and B , respectively; ω_k is the frequency of the waveguide field, which can be either linearly dependent on the amplitude of the wave vector k or linearizable around the frequency ω_0 . Having in mind that the total excitation number is conserved [due to the rotating-wave approximation used in Eq. (4)], the state of the model in the single-excitation subspace can be written as

$$|\psi(t)\rangle = \int dk c_k(t) a_k^\dagger e^{-i\omega_k t} |G\rangle + [u_A(t) \sigma_A^+ + u_B(t) \sigma_B^+] e^{-i\omega_0 t} |G\rangle, \quad (5)$$

where c_k is the probability amplitude of creating a photon with wave vector k in the waveguide; u_A and u_B

are the excitation amplitudes of atoms A and B , respectively; $|G\rangle$ denotes that the atoms are in the ground states and there is no photon in the waveguide. Solving the Schrödinger equation with Eqs. (1)-(5), one has

$$\dot{u}_A = -i \int dk g(t) (1 + e^{2ikd}) c_k e^{-i(\omega_k - \omega_0)t}, \quad (6)$$

$$\dot{u}_B = -i\Delta u_B - i \int dk g_0 (e^{ikd} + e^{3ikd}) \times c_k e^{-i(\omega_k - \omega_0)t}, \quad (7)$$

$$\dot{c}_k = -i [g(t) (1 + e^{-2ikd}) u_A + g_0 (e^{-ikd} + e^{-3ikd}) u_B] e^{i(\omega_k - \omega_0)t}. \quad (8)$$

By substituting the formal solution of the field amplitude (assuming that the waveguide is initially in the vacuum state)

$$c_k(t) = -i \int_0^t dt' [g(t') (1 + e^{-2ikd}) u_A(t') + g_0 (e^{-ikd} + e^{-3ikd}) u_B(t')] e^{i(\omega_k - \omega_0)t'} \quad (9)$$

into Eqs. (6) and (7), one can obtain the time-delayed dynamical equations (see Appendix A for more details)

$$\dot{u}_A = -\frac{2\pi g(t)}{v_g} [2g(t)u_A + 2g(t-2\tau)D_{A,2} + 3g_0 D_{B,1} + g_0 D_{B,3}], \quad (10)$$

$$\dot{u}_B = -i\Delta u_B - \frac{2\pi g_0}{v_g} [2g_0 u_B + 2g_0 D_{B,2} + 3g_0(t-\tau)D_{A,1} + g(t-3\tau)D_{A,3}], \quad (11)$$

where $D_{j,l} = \exp(il\phi) u_j(t-l\tau) \Theta(t-l\tau)$ ($j = A, B, \dots$ and $l = 1, 2, 3$) with $\phi = k_0 d$ and $\tau = d/v_g$ being the phase accumulation and the propagation time (time delay) of a photon traveling between adjacent coupling points, respectively; $\Theta(x)$ is the Heaviside step function.

III. DFI IN THE MARKOVIAN REGIME

Equations (10) and (11) describe the non-Markovian dynamics of the two giant atoms, revealing that the retardation effect depends on not only the coupling strength $g(t)$ at the present but also its values $g(t - l\tau)$ at early moments. The multiple retardations make the dynamics of the system a bit complicated. However, if τ is negligible compared to all the other characteristic time scales (Markovian regime), Eqs. (10) and (11) can be simplified to

$$\begin{aligned} \dot{u}_A &= -\frac{4\pi g(t)^2}{v_g} (1 + e^{2i\phi}) u_A \\ &\quad - \frac{2\pi g(t)g_0}{v_g} (3e^{i\phi} + e^{3i\phi}) u_B, \end{aligned} \quad (12)$$

$$\begin{aligned} \dot{u}_B &= -i\Delta u_B - \frac{4\pi g_0^2}{v_g} (1 + e^{2i\phi}) u_B \\ &\quad - \frac{2\pi g(t)g_0}{v_g} (3e^{i\phi} + e^{3i\phi}) u_A. \end{aligned} \quad (13)$$

Clearly, both atoms are dissipationless and their effective interaction is purely coherent when $\phi = (m + 1/2)\pi$ (m is an arbitrary integer). Now we consider cosine-type time-dependent couplings for atom A , i.e.,

$$g(t) = \Delta_g \cos(\Omega t + \theta) \quad (14)$$

with Δ_g , Ω , and θ being the amplitude, frequency, and initial phase of the modulation, respectively. If $\Omega = \Delta \gg 2\pi\Delta_g g_0/v_g$ and using the transformation $u_j \rightarrow u_j \exp(-i\Delta t)$, Eqs. (12) and Eq. (13) become

$$\dot{u}_A = -iG_m e^{i\theta} u_B, \quad (15)$$

$$\dot{u}_B = -iG_m e^{-i\theta} u_A, \quad (16)$$

where $\phi = (m + 1/2)\pi$ has been assumed and $G_m = (-1)^m 2\pi\Delta_g g_0/v_g$. One can see from Eqs. (15) and (16) that the modulation phase θ is encoded into the DFI between atoms A and B , mimicking a synthetic magnetic flux for photons transferring in between. Although the coupling phase θ can be gauged away for such a two-atom model (thus it has no particular interest in this case), it can significantly affect the dynamics of the system when a third atom is introduced to form a closed-loop trimer [22, 42, 45, 46], as will be shown below.

Although the above analysis is only applicable in the single-excitation subspace, the decoherence-free nature of our model can also be illustrated resorting to the theory of effective Hamiltonian [29, 47, 48]. As shown in Appendix B, in the Markovian regime, the effective Hamiltonian of the giant-atom dimer can be given by

$$H_{\text{eff,dim}} = G_m e^{i\theta} \sigma_B^\dagger \sigma_A + \text{H.c.}, \quad (17)$$

which shows a complex DFI between atoms A and B . Moreover, we have checked that the average interaction between the giant atoms and the waveguide field vanishes (thus the atoms are dissipationless) in this case.

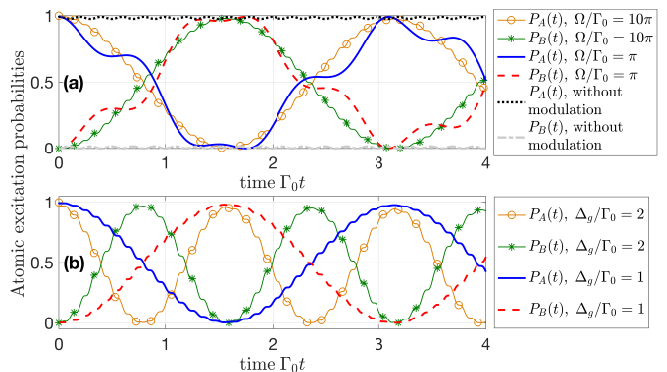


FIG. 2. Dynamics of atomic excitation probabilities $P_A(t)$ and $P_B(t)$ with different values of (a) modulation frequency Ω and (b) modulation amplitude Δ_g . We assume $\Delta_g/\Gamma_0 = 1$ in panel (a) and $\Omega/\Gamma_0 = 10\pi$ in panel (b). Moreover, we set $\Delta = \Omega$ for all lines, except for the case “without modulation” in panel (a): $\Omega = 0$ and $\Delta/\Gamma_0 = 10\pi$ in this case. Other parameters are $\Gamma_0 = 2\pi g_0^2/v_g$, $\phi = \pi/2$, $\theta = 0$, $\tau\Gamma_0 = 0.001$, and $|\psi(t=0)\rangle = \sigma_A^\dagger|G\rangle$.

Before proceeding, we briefly discuss the influence of the non-Markovian retardation effect on the result above. It is clear from Eqs. (10) and (11) that the retardation effect arising from the non-negligible propagation time τ may smear the DFI (such that the atoms are not perfectly dissipationless) and makes the dynamics much more complicated. To mitigate this detrimental effect, one can either consider a small enough τ , or assume $\Omega\tau = 2m\pi$ such that the atoms can still exhibit long-lived populations [49].

IV. DYNAMICS WITH EFFECTIVE DECOHERENCE-FREE INTERACTIONS

In this section we would like to verify the above results by numerically solving the time-delayed dynamical equations (10) and (11) with appropriate parameters. For clarification, we use $\Gamma_0 = 2\pi g_0^2/v_g$ (which is the radiative decay rate of atom B at each coupling point) as the unit of energies, and define $P_A(t) = |u_A(t)|^2$ and $P_B(t) = |u_B(t)|^2$ as the excitation probabilities of atoms A and B , respectively. Since we focus on the DFI of the giant atoms, we will always assume $\phi = \pi/2$ (i.e., $m = 0$) and $\tau\Gamma_0 \ll 1$.

Figure 2(a) shows the time evolutions of $P_A(t)$ and $P_B(t)$ with the initial state $|\psi(t=0)\rangle = \sigma_A^\dagger|G\rangle$ (atom A is initially excited) and different values of modulation frequency Ω . As discussed above, $\Omega = \Delta \gg |G_m|$ is required to justify the rotating-wave approximation [i.e., dropping high-frequency terms as in Eqs. (15) and (16)]. Indeed, we find that the two atoms exhibit a nearly decoherence-free excitation exchange (Rabi-like oscillation) when Ω is large enough (see, e.g., the orange line with circles and the green line with stars), while the dynamics deviate markedly from this typical form when Ω is small (see,

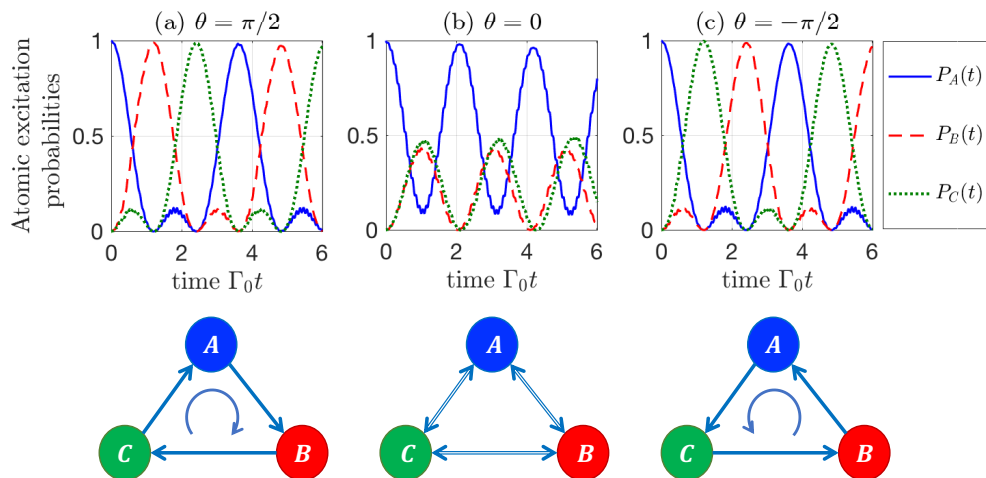


FIG. 3. Dynamics of atomic excitation probabilities $P_A(t)$, $P_B(t)$, and $P_C(t)$ in the atomic trimer [Fig. 1(b)] with different values of modulation phase θ . The lower plots illustrate the excitation transfer in the trimer, corresponding to panels (a)-(c), respectively. Other parameters are $\Gamma_0 = 2\pi g_0^2/v_g$, $\phi = \pi/2$, $\Delta/\Gamma_0 = \Omega/\Gamma_0 = 10\pi$, $\Delta_g/\Gamma_0 = 1$, $\tau\Gamma_0 = 0.001$, and $|\psi(t=0)\rangle = \sigma_A^+|G\rangle$.

e.g., the blue solid and red dashed lines). The Rabi-like line shapes exhibit additional tiny oscillations (thus we refer to them as “Rabi-like”) due to the cosine-type coupling modulations. Note that the interatomic interaction almost disappears and atom A exhibits a long-lived population in the absence of modulations (in this case we assume $\Omega = 0$ and $\Delta/\Gamma_0 = 10\pi$ instead). This is intuitive since the two atoms have very different transition frequencies. From this point of view, the coupling modulation allows for protected interactions between *detuned* atoms, which is physically important on its own.

We also plot in Fig. 2(b) the time evolutions of the atomic excitation probabilities with different values of modulation amplitude. It shows that the Rabi-like oscillation becomes faster for larger Δ_g since the effective coupling strength G_m between the two atoms is proportional to Δ_g . This thus provides an in-situ tunable scheme to manipulate the interactions between remote quantum emitters.

V. PHOTONIC AHARONOV-BOHM EFFECT IN GIANT-ATOM TRIMERS

As discussed in Sec. III, the effective coupling phase θ between atoms A and B has no actual physical meaning since it can always be gauged away (indeed, such a coupling phase is sensitive to the choice of the initial time). In view of this, we consider an additional two-level atom (labeled as atom C with the corresponding excitation amplitude u_C) coupled directly to A and B forming a closed-loop trimer, as shown in Fig. 1(b). To be specific, we assume: (i) atom C is resonant with atom B (thus it is detuned from atom A by Δ); (ii) atom C is coupled to atom A with a time-dependent coupling strength $\lambda(t) = 2G_0 \cos(\Omega t)$ and to atom B with a constant cou-

pling strength G_0 ($G_0 := G_{m=0}$). Consider the assumptions above, the dynamical equations of the trimer can be immediately obtained as

$$\dot{u}_A = -\frac{4\pi g^2(t)}{v_g} u_A - \frac{4\pi g(t)g(t-2\tau)}{v_g} D_{A,2} - \frac{2\pi g(t)g_0}{v_g} (3D_{B,1} + D_{B,3}) - i\lambda(t)u_C, \quad (18)$$

$$\dot{u}_B = -i\Delta u_B - \frac{4\pi g_0^2}{v_g} (u_B + D_{B,2}) - iG_0 u_C - \frac{2\pi g_0}{v_g} [3g(t-\tau)D_{A,1} + g(t-3\tau)D_{A,3}], \quad (19)$$

$$\dot{u}_C = -i\Delta u_C - i[\lambda(t)u_A + G_0 u_B]. \quad (20)$$

In the following of this section, we will demonstrate how the coupling phase θ affects the single-excitation dynamics of the trimer.

Figure 3 shows the dynamics governed by Eqs. (18)-(20) [we define $P_C(t) = |u_C(t)|^2$ as the excitation probability of atom C], with the initial state $|\psi(t=0)\rangle = \sigma_A^+|G\rangle$ and different values of θ . It shows that the phase θ plays a key role in this case. The three atoms constitute an effective Aharonov-Bohm cage [50] (i.e., a closed-loop plaquette threaded by a magnetic field), such that it exhibits asymmetric excitation transfer if θ is not an integer multiple of π . In particular, as shown in Figs. 3(a) and 3(c), directional excitation circulation [42] can be observed if $\text{mod}(\theta, \pi) = \pi/2$, with the circulation direction determined by the sign of θ (or say, by whether the subscript integer m of G_m is odd or even). In principle, the excitation transfer should be symmetric if $\text{mod}(\theta, \pi) = 0$. However, as shown in Fig. 3(b), there is a minor difference between the time evolutions of $P_B(t)$ and $P_C(t)$, which we conclude arises from the finite retardation effect between atoms A and B . We have checked that such a difference tends to vanish as τ decreases gradually.

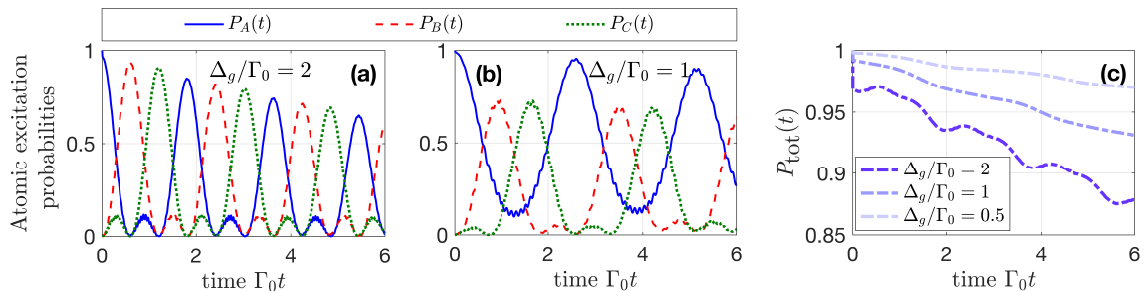


FIG. 4. (a, b) Dynamics of atomic excitation probabilities $P_A(t)$, $P_B(t)$, and $P_C(t)$ in the atomic trimer [Fig. 1(c)] with (a) $\Delta_g/\Gamma_0 = 2$ and (b) $\Delta_g/\Gamma_0 = 1$. (c) Dynamics of total excitation probability $P_{\text{tot}}(t)$ in the atomic trimer [Fig. 1(c)] with different values of Δ_g . Other parameters are $\Gamma_0 = 2\pi g_0^2/v_g$, $\phi = \pi/2$, $\Delta/\Gamma_0 = \Omega/\Gamma_0 = 10\pi$, $\theta = \pi/2$, $\tau\Gamma_0 = 0.001$, and $|\psi(t=0)\rangle = \sigma_A^+|G\rangle$.

Note that the direct interactions between atom C and the others impose some limitations on the architecture of the model. For example, atoms A and B have to be spatially close in order to interact directly with atom C . In view of this, we would like to extend the above trimer to a purely giant-atom version, where all the three atoms interact with each other via waveguide-mediated DFIs. As shown in Fig. 1(c), atoms A and C exhibit a DFI through the upper waveguide, while the DFIs between them and atom B are mediated by the lower waveguide. In particular, atoms B and C are coupled to the waveguides with identical and constant strength g_0 , while atom A is coupled to the lower and upper waveguides with different time-dependent coupling strengths $g(t)$ and $g'(t)$, respectively (for each waveguide the two couplings of A are identical). For simplicity, we still assume that the coupling points are equally spaced by distance d [in the lower waveguide, atoms A and C share a common coupling point as shown in Fig. 1(c)].

The time-delayed dynamical equations of this model are given in Appendix C [see Eqs. (C1)-(C3)], which, under certain conditions, show a protected all-to-all interaction (i.e., all the atoms interact with each other via DFIs). One may argue that the protected all-to-all interaction can also be realized by using only one waveguide as shown in Fig. 1(d) [27]. However, we do not concentrate on this model since the global coupling phase (i.e., the total synthetic magnetic flux threading the closed-loop trimer) is always zero in this case (see Appendix C for more details). Hereafter, we assume $g(t) = \Delta_g \cos(\Omega t + \theta)$ and $g'(t) = \Delta_g \cos(\Omega t)$ for the model in Fig. 1(c) to demonstrate the photonic Aharonov-Bohm effect (in this case θ plays the role of global coupling phase).

We plot in Figs. 4(a) and 4(b) the time evolutions of the atomic excitation probabilities in such a giant-atom trimer with $\theta = \pi/2$. Similar to that in Fig. 3(a), the single excitation initialized in atom A “hops” directionally in sequence of $A \rightarrow B \rightarrow C \rightarrow A$, yet the damping of the total excitation probability $P_{\text{tot}}(t) = P_A(t) + P_B(t) + P_C(t)$ is enhanced due to the stronger retardation effect in this model. On one hand, as shown in

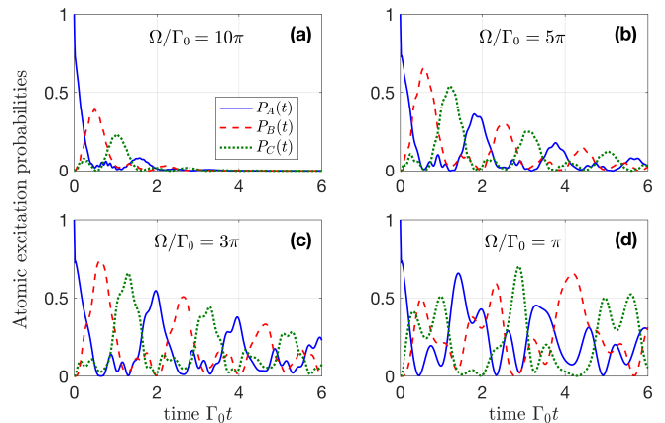


FIG. 5. Dynamics of atomic excitation probabilities $P_A(t)$, $P_B(t)$, and $P_C(t)$ in the atomic trimer [Fig. 1(c)] with (a) $\Omega/\Gamma_0 = 10\pi$, (b) $\Omega/\Gamma_0 = 5\pi$, (c) $\Omega/\Gamma_0 = 3\pi$, and (d) $\Omega/\Gamma_0 = \pi$. All panels in this figure share the same legend. Other parameters are $\Gamma_0 = 2\pi g_0^2/v_g$, $\Delta = \Omega$, $\phi = \pi/2$, $\alpha/\Gamma_0 = 2$, $\theta = \pi/2$, $\tau\Gamma_0 = 0.01$, and $|\psi(t=0)\rangle = \sigma_A^+|G\rangle$.

Fig. 4(c), $P_{\text{tot}}(t)$ shows a slower damping for smaller Δ_g since the effective decay rate of atom A [described by the first two terms on the right side of Eq. (C1)] decreases gradually as Δ_g goes to zero. On the other hand, by comparing Figs. 4(a) and 4(b) one can find that the effective coupling strength between atom A and the others (which affects the transfer efficiency and the period of the circulation) can be controlled by tuning the modulation amplitude Δ_g .

Finally, we would like to demonstrate the influence of a stronger retardation effect on the present results and discuss how to mitigate this effect in some sense by tuning the modulation parameters. For relatively large τ , as shown in Fig. 5(a), the total excitation probability becomes strongly damped and falls to zero rapidly, although the directional excitation circulation can still be observed. Such a rapid damping, however, can be weakened by using smaller modulation frequency as shown in Figs. 5(b) and 5(c) ($\Delta = \Omega$ is always satisfied). This phenomenon can be understood again from the effec-

tive decay rate of atom A : as shown in Eq. (C1), atom A can be finally dissipationless if $g(t) = g(t - 2\tau)$ and $g'(t) = g'(t - 2\tau)$ [i.e., $\text{mod}(\Omega\tau, \pi) = 0$], while its decay cannot be completely suppressed if $0 < \text{mod}(\Omega\tau, \pi) \ll \pi$. However, decreasing the value of Ω also smears the Aharonov-Bohm effect since the anti-rotating-wave terms (i.e., the high-frequency oscillating terms in the effective Hamiltonian and dynamical equations) come into play eventually. As shown in Fig. 5(d), the directional excitation circulation almost disappears for small enough Ω . In other words, there is a tradeoff between the retardation-induced dissipation and the effect of synthetic magnetic field in this case.

VI. CONCLUSIONS

In summary, we have demonstrated how to create a synthetic magnetic field for the effective decoherence-free Hamiltonians of giant atoms resorting to periodic coupling modulations and suitable arrangements of atom-waveguide coupling points. With our scheme one can not only realize DFIs between detuned giant atoms, but also observe the photonic Aharonov-Bohm effect in closed-loop chains of giant atoms. Moreover, we have considered the non-Markovian retardation effect and studied its influence on the atomic dynamics. The retardation effect does not denature the Aharonov-Bohm effect and the resulting dissipation can be controlled via the modulation parameters within a certain range.

In principle, the synthetic magnetic field can also be created by modulating the transition frequency of the giant atom. For example, recalling the giant-atom dimer in Fig. 1(a), one can assume constant and uniform couplings for both two atoms and a time-dependent detuning for atom B . Then a DFI between the two atoms can be real-

ized under certain conditions, as shown in Appendix D. However, the coupling-modulation scheme shows two major advantages over the frequency-modulation one [45]: (i) the requirements for the rotating-wave approximation to be valid in the coupling-modulation scheme are less severe; (ii) for the frequency-modulation scheme, there are many sidebands that cannot be neglected in many cases (especially when multiple frequency modulations are considered or a relatively faster modulation is employed), which may smear the DFI. In view of this, we focus on the coupling-modulation scheme in this paper.

The results in this paper can be applied for many applications and further investigations. For example, our scheme highlights a way towards quantum simulations of many-body systems that are subject to various gauge fields and towards engineering more high-fidelity quantum gates [27, 28]. It is also possible to generate fractional quantum Hall states of light by simply increasing the size of our models (e.g., implementing two-dimensional square or quasi-one-dimensional ladder lattices of giant atoms with tailored couplings) [42]. Although in this paper we have concentrated on models made up of superconducting qubits and microwave transmission lines, our proposal is general and can be immediately extended to other possible setups, such as quantum emitters coupled to real and synthetic discrete lattices. Moreover, the synthetic gauge field offers the opportunity of implementing richer topological phases based on the effective spin Hamiltonians of giant atoms [5].

ACKNOWLEDGMENTS

We would like to thank F. Ciccarello, Y. Zhang and Y.-T. Chen for helpful discussions. This work was supported by the National Natural Science Foundation of China (under Grants No. 12074030 and No. 12274107).

Appendix A: Time-delayed dynamical equations of the giant-atom dimer

By substituting Eq. (9) into Eqs. (6) and (7), we have

$$\begin{aligned} \dot{u}_A(t) = & - \int_0^t dt' \int_{-\infty}^{+\infty} dk e^{-i(\omega_k - \omega_0)(t-t')} \{ 2g(t)g(t') [1 + \cos(2kd)] u_A(t') \\ & + g(t)g_0 (e^{ikd} + 2e^{-ikd} + e^{-3ikd}) u_B(t') \}, \end{aligned} \quad (\text{A1})$$

$$\begin{aligned} \dot{u}_B(t) = & -i\Delta u_B(t) - \int_0^t dt' \int_{-\infty}^{+\infty} dk e^{-i(\omega_k - \omega_0)(t-t')} \{ 2g_0^2 [1 + \cos(2kd)] u_B(t') \\ & + g(t')g_0 (2e^{ikd} + e^{-ikd} + e^{3ikd}) u_A(t') \}. \end{aligned} \quad (\text{A2})$$

If we change the integration variable as $\int_{-\infty}^{+\infty} dk f(k) \rightarrow \int_0^{+\infty} d\omega_k [f(k) + f(-k)]/v_g$ and write the dispersion relation of the waveguide as $\omega_k = \omega_0 + \nu_k = \omega_0 + (k - k_0)v_g$ [51, 52], with k_0 the wave vector corresponding to frequency ω_0

and v_g the group velocity of photons in the waveguide, Eqs. (A1) and (A2) become

$$\begin{aligned}\dot{u}_A(t) &= -\frac{1}{v_g} \int_0^t dt' \int_{-\infty}^{+\infty} d\nu_k e^{-i\nu_k(t-t')} \{4g(t)g(t')[1 + \cos(2kd)]u_A(t') \\ &\quad + g(t)g_0(3e^{ikd} + 3e^{-ikd} + e^{3ikd} + e^{-3ikd})u_B(t')\}, \\ &= -\frac{2\pi}{v_g} \int_0^t dt' \{2g(t)g(t') [2\delta(t-t') + e^{2i\phi}\delta(t-t'-2\tau)]u_A(t') \\ &\quad + g(t)g_0 [3e^{i\phi}\delta(t-t'-\tau) + e^{3i\phi}\delta(t-t'-3\tau)]u_B(t')\},\end{aligned}\tag{A3}$$

$$\begin{aligned}\dot{u}_B(t) &= -i\Delta u_B(t) - \frac{1}{v_g} \int_0^t dt' \int_{-\infty}^{+\infty} d\nu_k e^{-i\nu_k(t-t')} \{4g_0^2[1 + \cos(2kd)]u_B(t') \\ &\quad + g(t')g_0(3e^{ikd} + 3e^{-ikd} + e^{3ikd} + e^{-3ikd})u_A(t')\} \\ &= -i\Delta u_B(t) - \frac{2\pi}{v_g} \int_0^t dt' \{2g_0^2 [2\delta(t-t') + e^{2i\phi}\delta(t-t'-2\tau)]u_B(t') \\ &\quad + g(t')g_0 [3e^{i\phi}\delta(t-t'-\tau) + e^{3i\phi}\delta(t-t'-3\tau)]u_A(t')\},\end{aligned}\tag{A4}$$

where $\phi = k_0d$ and $\tau = d/v_g$. In the last steps of Eqs. (A3) and (A4), we have omitted the time-advanced terms containing $\delta(t-t'+l\tau)$ ($l = 1, 2, 3$) since they do not contribute to the integral $\int_0^t(\dots)dt'$. Finally, one can obtain the time-delayed dynamical equations (10) and (11) by using the sifting property $\int dt f(t)\delta(t-t') = f(t')$ of delta functions.

Appendix B: Effective Hamiltonian

In this appendix we would like to demonstrate the decoherence-free mechanism of the giant-atom dimer in Fig. 1(a) by deriving its effective Hamiltonian. We first consider a more general situation where a set of two-level giant atoms are coupled to a common waveguide with arbitrary arrangements of coupling points. Similar to the models studied in this paper, one of the atoms (with transition frequency ω_0 ; labeled as atom A) is detuned from the others by Δ and coupled to the waveguide with time-dependent coupling strength $g(t)$, while the other giant atoms have the same transition frequency ($\omega_0 + \Delta$) and are coupled to the waveguide with constant coupling strength g_0 . In this case, the Hamiltonian in the interaction picture can be written as

$$\begin{aligned}V(t) &= \int_{-\infty}^{+\infty} dk \left[g(t) (e^{-ikx_{A1}} + e^{-ikx_{A2}}) \sigma_{AA} a_k^\dagger e^{i(\Delta_k + \Delta)t} + g_0 \sum_{j,l} e^{-ikx_{jl}} \sigma_j a_k^\dagger e^{i\Delta_k t} + \text{H.c.} \right] \\ &= \int_{-\infty}^{+\infty} dk \left\{ g(t) [e^{-i\varphi_{A1}} e^{i\Delta_k(t-\tau_{A1})} + e^{-i\varphi_{A2}} e^{i\Delta_k(t-\tau_{A2})}] \sigma_{AA} a_k^\dagger e^{-i\Delta t} + g_0 \sum_{j,l} e^{-i\varphi_{jl}} \sigma_j a_k^\dagger e^{i\Delta_k(t-\tau_{jl})} + \text{H.c.} \right\},\end{aligned}\tag{B1}$$

where $\Delta_k = \omega_k - \omega_0 - \Delta$. x_{jl} is the position of the l th coupling point of atom j , with which we define $\tau_{jl} = x_{jl}/v_g$ and $\varphi_{jl} = k_0x_{jl}$. In the second step of Eq. (B1) we have used the linearized dispersion relation $\omega_k = \omega_0 + (k - k_0)v_g$. If we consider a discrete time axis $t_n = nT$ with the time interval T short enough compared with the characteristic time of interaction, the average interaction can be defined as [29, 48]

$$\bar{V} = \frac{1}{T} \int_{t_{n-1}}^{t_n} ds V(s),\tag{B2}$$

and the effective Hamiltonian of the giant atoms can be given by

$$H_{\text{eff}} = \frac{-i}{2T} \int_{t_{n-1}}^{t_n} ds \int_{t_{n-1}}^s ds' [V(s), V(s')].\tag{B3}$$

To realize decoherence-free Hamiltonians, it is necessary to fulfill the condition $\bar{V} = 0$. Now if we consider the giant-atom dimer in Fig. 1(a) with cosine-type time-dependent couplings $g(t) = \Delta_g \cos(\Delta t + \theta)$ for atom A , Eq. (B1)

becomes

$$V(t) = \int_{-\infty}^{+\infty} dk \left\{ \frac{\Delta g}{2} \left[e^{i\Delta_k t} + e^{-2i\phi} e^{i\Delta_k(t-2\tau)} \right] (e^{i\theta} + e^{-2i\Delta t} e^{-i\theta}) \sigma_A a_k^\dagger + g_0 \left[e^{-i\phi} e^{i\Delta_k(t-\tau)} + e^{-3i\phi} e^{i\Delta_k(t-3\tau)} \right] \sigma_B a_k^\dagger + \text{H.c.} \right\}, \quad (\text{B4})$$

where we have assumed $\{x_{A1}, x_{B1}, x_{A2}, x_{B2}\} = \{0, d, 2d, 3d\}$ such that $\phi = k_0 d$ and $\tau = d/v_g$ as defined in the main text. Substituting Eq. (B4) into Eq. (B3) we can obtain the effective Hamiltonian of the giant-atom dimer, i.e.,

$$\begin{aligned} H_{\text{eff,dim}} &= \frac{-i}{2T} \frac{2\pi\Delta g g_0}{v_g} \int_{t_{n-1}}^{t_n} ds \int_{t_{n-1}}^s ds' \left\{ \left[2e^{i\phi} [\delta(s' - s + \tau) - \delta(s - s' + \tau)] \right. \right. \\ &\quad \left. \left. + e^{3i\phi} [\delta(s' - s + 3\tau) - \delta(s - s' + 3\tau)] + e^{-i\phi} [\delta(s' - s - \tau) - \delta(s - s' - \tau)] \right] e^{i\theta} \sigma_B^\dagger \sigma_A + \text{H.c.} \right\} \\ &= \frac{-i\pi\Delta g g_0}{v_g} \left[(2e^{i\phi} + e^{3i\phi} - e^{-i\phi}) e^{i\theta} \sigma_B^\dagger \sigma_A + \text{H.c.} \right], \end{aligned} \quad (\text{B5})$$

where we have assumed that all the time delays $l\tau$ are negligible compared to T (Markovian regime) and have dropped the high-frequency oscillating terms containing $\exp(-2i\Delta t)$. When $\phi = (m+1/2)\pi$, the effective Hamiltonian becomes

$$H_{\text{eff,dim}} = G_m e^{i\theta} \sigma_B^\dagger \sigma_A + \text{H.c.} \quad (\text{B6})$$

with $G_m = (-1)^m 2\pi\Delta g g_0/v_g$, which shows a complex DFI between atoms A and B . Moreover, one can see from Eqs. (B2) and (B4) that the average interaction between the giant atoms and the waveguide field vanishes (i.e., $\bar{V} = 0$) in this case.

Appendix C: Dynamical equations of the model in Figs. 1(c) and 1(d)

For the giant-atom trimer in Fig. 1(c), the time-delayed dynamical equations of the atomic excitation amplitudes can be immediately given by

$$\begin{aligned} \dot{u}_A &= -\frac{4\pi[g^2(t) + g'^2(t)]}{v_g} u_A - \frac{4\pi[g(t)g(t-2\tau) + g'(t)g'(t-2\tau)]}{v_g} D_{A,2} - \frac{2\pi g(t)g_0}{v_g} (3D_{B,1} + D_{B,3}) \\ &\quad - \frac{2\pi g(t)g_0}{v_g} (u_C + 2D_{C,2} + D_{C,4}) - \frac{2\pi g'(t)g_0}{v_g} (3D_{C,1} + D_{C,3}), \end{aligned} \quad (\text{C1})$$

$$\begin{aligned} \dot{u}_B &= -i\Delta u_B - \frac{4\pi g_0^2}{v_g} (u_B + D_{B,2}) - \frac{6\pi g(t-\tau)g_0}{v_g} D_{A,1} - \frac{2\pi g(t-3\tau)g_0}{v_g} D_{A,3} \\ &\quad - \frac{2\pi g_0^2}{v_g} (3D_{C,1} + D_{C,3}), \end{aligned} \quad (\text{C2})$$

$$\begin{aligned} \dot{u}_C &= -i\Delta u_C - \frac{8\pi g_0^2}{v_g} (u_C + D_{C,2}) - \frac{2\pi g(t)g_0}{v_g} u_A - \frac{4\pi g(t-2\tau)g_0}{v_g} D_{A,2} - \frac{2\pi g(t-4\tau)g_0}{v_g} D_{A,4} \\ &\quad - \frac{6\pi g'(t-\tau)g_0}{v_g} D_{A,1} - \frac{2\pi g'(t-3\tau)g_0}{v_g} D_{A,3} - \frac{2\pi g_0^2}{v_g} (3D_{B,1} + D_{B,3}). \end{aligned} \quad (\text{C3})$$

which can be simplified to

$$\dot{u}_A = -i \frac{4\pi g(t)g_0}{v_g} u_B - i \frac{4\pi g'(t)g_0}{v_g} u_C, \quad (\text{C4})$$

$$\dot{u}_B = -i\Delta u_B - i \frac{4\pi g(t)g_0}{v_g} u_A - i \frac{4\pi g_0^2}{v_g} u_C, \quad (\text{C5})$$

$$\dot{u}_C = -i\Delta u_C - i \frac{4\pi g'(t)g_0}{v_g} u_A - i \frac{4\pi g_0^2}{v_g} u_B, \quad (\text{C6})$$

if $\phi = \pi/2$ and $\tau \rightarrow 0$. By assuming cosine-type couplings $g(t) = \Delta_g \cos(\Omega t + \theta)$ and $g'(t) = \Delta_g \cos(\Omega t)$ for atom A with $\Omega \equiv \Delta$, one finally has

$$\dot{u}_A = -iG_0 e^{i\theta} u_B - iG_0 u_C, \quad (\text{C7})$$

$$\dot{u}_B = -iG_0 e^{-i\theta} u_A - 2i\Gamma_0 u_C, \quad (\text{C8})$$

$$\dot{u}_C = -iG_0 u_A - 2i\Gamma_0 u_B, \quad (\text{C9})$$

which shows a protected all-to-all interaction with synthetic magnetic flux θ .

As mentioned in the main text, the protected all-to-all interaction among atoms A , B , and C can also be implemented by using only one waveguide, provided that the coupling points of the three atoms are arranged according to the configuration in Fig. 1(d). In this case, we assume that the coupling points are equally spaced by d' such that the phase accumulation (propagation time) of the field between adjacent coupling points becomes $\phi' = k_0 d'$ ($\tau' = d'/v_g$). Again, atoms B and C are coupled to the waveguide with identical and constant strength g_0 , while atom A interacts with the waveguide with time-dependent strength $g(t)$ at each coupling point. After some algebra, the dynamical equations of the model can be obtained as

$$\dot{u}_A = -\frac{2\pi g(t)}{v_g} [2g(t)u_A + 2g(t - 3\tau')D'_{A,3} + g_0 (2D'_{B,1} + D'_{B,2} + D'_{B,4} + D'_{C,1} + 2D'_{C,2} + D'_{C,5})], \quad (\text{C10})$$

$$\begin{aligned} \dot{u}_B = & -i\Delta u_B - \frac{2\pi g_0}{v_g} [2g_0 u_B + 2g_0 D'_{B,3} + 2g(t - \tau')D'_{A,1} + g(t - 2\tau')D'_{A,2} \\ & + g(t - 4\tau')D'_{A,4} + g_0 (2D'_{C,1} + D'_{C,2} + D'_{C,4})], \end{aligned} \quad (\text{C11})$$

$$\begin{aligned} \dot{u}_C = & -i\Delta u_C - \frac{2\pi g_0}{v_g} [2g_0 u_C + 2g_0 D'_{C,3} + g(t - \tau')D'_{A,1} + 2g(t - 2\tau')D'_{A,2} \\ & + g(t - 5\tau')D'_{A,5} + g_0 (2D'_{B,1} + D'_{B,2} + D'_{B,4})], \end{aligned} \quad (\text{C12})$$

where $D'_{j,l} = \exp(il\phi')u_j(t - l\tau')\Theta(t - l\tau')$. When $\phi' = (2m + 1/3)\pi$ and $\tau \rightarrow 0$, the above three equations become

$$\dot{u}_A = -i\frac{4\pi g(t)g_0}{v_g} \sin\left(\frac{\pi}{3}\right)u_B - i\frac{4\pi g(t)g_0}{v_g} \sin\left(\frac{\pi}{3}\right)u_C, \quad (\text{C13})$$

$$\dot{u}_B = -i\Delta u_B - i\frac{4\pi g(t)g_0}{v_g} \sin\left(\frac{\pi}{3}\right)u_A - i\frac{4\pi g_0^2}{v_g} \sin\left(\frac{\pi}{3}\right)u_C, \quad (\text{C14})$$

$$\dot{u}_C = -i\Delta u_C - i\frac{4\pi g(t)g_0}{v_g} \sin\left(\frac{\pi}{3}\right)u_A - i\frac{4\pi g_0^2}{v_g} \sin\left(\frac{\pi}{3}\right)u_B, \quad (\text{C15})$$

which are identical with Eqs. (C4)-(C6) except for the modified effective coupling strengths. By assuming $g(t) = \Delta_g \cos(\Omega t + \theta)$ and performing the transformation $u_j \rightarrow u_j \exp(-i\Delta t)$, Eqs. (C13)-(C15) become

$$\dot{u}_A \simeq -iG' e^{i\theta} u_B - iG' e^{i\theta} u_C, \quad (\text{C16})$$

$$\dot{u}_B \simeq -iG' e^{-i\theta} u_A - 2i\Gamma' u_C, \quad (\text{C17})$$

$$\dot{u}_C \simeq -iG' e^{-i\theta} u_A - 2i\Gamma' u_B, \quad (\text{C18})$$

where $G' = G_0 \sin(\pi/3) = 2\pi g_0 \Delta_g \sin(\pi/3)/v_g$ and $\Gamma' = \Gamma_0 \sin(\pi/3) = 2\pi g_0^2 \sin(\pi/3)/v_g$. Clearly, the effective coupling phase can always be gauged away by the transformation $u_A \rightarrow u_A \exp(i\theta)$. Therefore the Aharonov-Bohm effect cannot be observed in this case.

Appendix D: Frequency-modulation scheme

In this appendix, we consider that atoms A and B (recalling the giant-atom dimer) are coupled to the waveguide in the braided manner, yet with constant and uniform couplings (coupling strength g_0) instead. While the transition frequency ω_0 of atom A is assumed to be constant, we consider a frequency modulation for atom B such that there is a small time-dependent detuning $\Delta_0 + \Delta(t)$ between the two atoms. In this case, the Hamiltonian of the model can be written as

$$H' = H'_a + H_w + H'_{\text{int}}, \quad (\text{D1})$$

$$H'_a = \omega_0 \sigma_A^+ \sigma_A^- + [\omega_0 + \Delta_0 + \Delta(t)] \sigma_B^+ \sigma_B^-, \quad (\text{D2})$$

$$\begin{aligned} H'_{\text{int}} = & \int dk g_0 [(1 + e^{2ikd}) \sigma_A^+ a_k \\ & + (e^{ikd} + e^{3ikd}) \sigma_B^+ a_k + \text{H.c.}], \end{aligned} \quad (\text{D3})$$

where H_w is identical with that in Eq. (3). With the single-excitation state of the system given in Eq. (5) and a similar calculation procedure as shown in the main text, one can obtain the dynamical equations of the atomic excitation amplitudes as

$$\dot{u}_A = -\Gamma_0 [2u_A + 2D_{A,2} + 3D_{B,1} + D_{B,3}], \quad (\text{D4})$$

$$\begin{aligned} \dot{u}_B = & -i[\Delta_0 + \Delta(t)]u_B - \Gamma_0 [2u_B \\ & + 2D_{B,2} + 3D_{A,1} + D_{A,3}], \end{aligned} \quad (\text{D5})$$

where $\Gamma_0 = 2\pi g_0^2/v_g$ and $D_{j,l} = \exp(il\phi)u_j(t - l\tau)\Theta(t - l\tau)$ as defined in the main text. Once again, in the Markovian regime with negligible time delays and if $\phi = \pi/2$, the above two equations can be simplified as

$$\dot{u}_A = -2i\Gamma_0 u_B, \quad (\text{D6})$$

$$\dot{u}_B = -i[\Delta_0 + \Delta(t)]u_B - 2i\Gamma_0 u_A. \quad (\text{D7})$$

Now we consider a cosine-type modulation $\Delta(t) = \Delta'_g \cos(\Omega't + \theta')$ (Δ'_g , Ω' , and θ' are the amplitude, fre-

quency, and initial phase of the modulation, respectively) for the detuning and and perform a transformation

$$u_B(t) \rightarrow u_B(t)e^{-i\Delta_0 t}e^{-i\chi \sin(\Omega' t + \theta')} \quad (\text{D8})$$

with $\chi = \Delta'_g/\Omega'$, Eqs. (D6) and (D7) become

$$\dot{u}_A = -2i\Gamma_0 u_B e^{-i\Delta_0 t}e^{-i\chi \sin(\Omega' t + \theta')}, \quad (\text{D9})$$

$$\dot{u}_B = -2i\Gamma_0 u_A e^{i\Delta_0 t}e^{i\chi \sin(\Omega' t + \theta')}. \quad (\text{D10})$$

Assuming $\Omega' = \Delta_0 \gg 2\Gamma_0$ and using the Jacobi-Anger expansion

$$e^{-iz \sin x} = \sum_{q=-\infty}^{+\infty} J_q(z) e^{-iqx}, \quad (\text{D11})$$

where $J_q(z)$ is the Bessel function of the first kind, one finally has

$$\dot{u}_A = -2i\Gamma_0 J_{-1}(\chi) u_B e^{i\theta'}, \quad (\text{D12})$$

$$\dot{u}_B = -2i\Gamma_0 J_{-1}(\chi) u_A e^{-i\theta'}. \quad (\text{D13})$$

Clearly, a complex DFI between atoms A and B can be created as well in this case.

-
- [1] A. F. Kockum, Quantum optics with giant atoms—the first five years, in *Mathematics for Industry* (Springer, Singapore, 2021), pp: 125-146.
- [2] A. F. Kockum, P. Delsing, and G. Johansson, Designing frequency-dependent relaxation rates and Lamb shifts for a giant artificial atom, *Phys. Rev. A* **90**, 013837 (2014).
- [3] L. Guo, A. Grimsmo, A. F. Kockum, M. Pletyukhov, and G. Johansson, Giant acoustic atom: A single quantum system with a deterministic time delay, *Phys. Rev. A* **95**, 053821 (2017).
- [4] L. Guo, A. F. Kockum, F. Marquardt, and G. Johansson, Oscillating bound states for a giant atom, *Phys. Rev. Res.* **2**, 043014 (2020).
- [5] X. Wang, T. Liu, A. F. Kockum, H.-R. Li, and F. Nori, Tunable Chiral Bound States with Giant Atoms, *Phys. Rev. Lett.* **126**, 043602 (2020).
- [6] W. Zhao and Z. Wang, Single-photon scattering and bound states in an atom-waveguide system with two or multiple coupling points, *Phys. Rev. A* **101**, 053855 (2020).
- [7] C. Vega, M. Bello, D. Porras, and A. González-Tudela, Qubit-photon bound states in topological waveguides with long-range hoppings, *Phys. Rev. A* **104**, 053522 (2021).
- [8] H. Xiao, L. Wang, Z.-H. Li, X. Chen, and L. Yuan, Bound state in a giant atom-modulated resonators system, *npj Quantum Info.* **8**, 80 (2022).
- [9] W. Cheng, Z. Wang, and Y.-x. Liu, Topology and retardation effect of a giant atom in a topological waveguide, *Phys. Rev. A* **106**, 033522 (2022).
- [10] C. Vega, D. Porras, and A. González-Tudela, Topological multi-mode waveguide QED, [arXiv:2207.02090](https://arxiv.org/abs/2207.02090).
- [11] K. H. Lim, W.-K. Mok, and L.-C. Kwek, Oscillating bound states in non-Markovian photonic lattices, [arXiv:2208.11097](https://arxiv.org/abs/2208.11097).
- [12] L. Du and Y. Li, Single-photon frequency conversion via a giant Λ -type atom, *Phys. Rev. A* **104**, 023712 (2021).
- [13] L. Du, Y.-T. Chen, and Y. Li, Nonreciprocal frequency conversion with chiral Λ -type atoms, *Phys. Rev. Res.* **3**, 043226 (2021).
- [14] Q. Y. Cai and W. Z. Jia, Coherent single-photon scattering spectra for a giant-atom waveguide-QED system beyond the dipole approximation, *Phys. Rev. Res.* **3**, 043226 (2021).
- [15] S. L. Feng and W. Z. Jia, Manipulating single-photon transport in a waveguide-QED structure containing two giant atoms, *Phys. Rev. A* **104**, 063712 (2021).
- [16] X.-L. Yin, Y.-H. Liu, J.-F. Huang, and J.-Q. Liao, Single-photon scattering in a giant-molecule waveguide-QED system, *Phys. Rev. A* **106**, 013715 (2022).
- [17] W. Zhao, Y. Zhang, and Z. Wang, Phase-modulated Autler-Townes splitting in a giant-atom system within waveguide QED, *Front. Phys.* **17**, 42506 (2022).
- [18] Y.-T. Chen, L. Du, L. Guo, Z. Wang, Y. Zhang, Y. Li, J.-H. Wu, Nonreciprocal and chiral single-photon scattering for giant atoms, *Commun. Phys.* **5**, 215 (2022).
- [19] Y. Zhu, R. Wu, and S. Xue, Spatial Non-Locality Induced Non-Markovian EIT in a Single Giant Atom, [arXiv:2106.05020](https://arxiv.org/abs/2106.05020).
- [20] G. Andersson, B. Suri, L. Guo, T. Aref, and P. Delsing, Non-exponential decay of a giant artificial atom, *Nat. Phys.* **15**, 1123 (2019).
- [21] S. Longhi, Photonic simulation of giant atom decay, *Opt. Lett.* **45**, 3017 (2020).
- [22] L. Du, M.-R. Cai, J.-H. Wu, Z. Wang, and Y. Li, Single-photon nonreciprocal excitation transfer with non-Markovian retarded effects, *Phys. Rev. A* **103**, 053701 (2021).
- [23] Q.-Y. Qiu, Y. Wu, and X.-Y. Lü, Collective Radiance of Giant Atoms in Non-Markovian Regime, [arXiv:2205.10982](https://arxiv.org/abs/2205.10982).
- [24] A. Soro, and A. F. Kockum, Chiral quantum optics with giant atoms, *Phys. Rev. A* **105**, 023712 (2022).
- [25] X. Wang and H.-R. Li, Chiral quantum network with giant atoms, *Quantum Sci. Technol.* **7**, 035007 (2022).
- [26] L. Du, Y. Zhang, J.-H. Wu, A. F. Kockum, and Y. Li, Giant Atoms in a Synthetic Frequency Dimension, *Phys. Rev. Lett.* **128**, 223602 (2022).
- [27] A. F. Kockum, G. Johansson, and F. Nori, Decoherence-Free Interaction between Giant Atoms in Waveguide Quantum Electrodynamics, *Phys. Rev. Lett.* **120**, 140404 (2018).
- [28] B. Kannan, M. Ruckriegel, D. Campbell, A. F. Kockum, J. Braumüller, D. Kim, M. Kjaergaard, P. Krantz, A. Melville, B. M. Niedzielski, A. Vepsäläinen, R. Winik, J. Yoder, F. Nori, T. P. Orlando, S. Gustavsson,

- and W. D. Oliver, Waveguide quantum electrodynamics with superconducting artificial giant atoms, *Nature (London)* **583**, 775-779 (2020).
- [29] A. Carollo, D. Cilluffo, and F. Ciccarello, Mechanism of decoherence-free coupling between giant atoms, *Phys. Rev. Res.* **2**, 043184 (2020).
- [30] E. Shahmoon and G. Kurizki, Nonradiative interaction and entanglement between distant atoms, *Phys. Rev. A* **87**, 033831 (2013).
- [31] J. S. Douglas, H. Habibian, C.-L. Hung, A. V. Gorshkov, H. J. Kimble, and D. E. Chang, Quantum many-body models with cold atoms coupled to photonic crystals, *Nat. Photon.* **9**, 326 (2015).
- [32] D. E. Chang, J. S. Douglas, A. González-Tudela, C.-L. Hung, and H. J. Kimble, Colloquium: Quantum matter built from nanoscopic lattices of atoms and photons, *Rev. Mod. Phys.* **90**, 031002 (2018).
- [33] Y. Aharonov and D. Bohm, Significance of Electromagnetic Potentials in the Quantum Theory, *Phys. Rev.* **115**, 485 (1959).
- [34] R. O. Umucalılar and I. Carusotto, Artificial gauge field for photons in coupled cavity arrays, *Phys. Rev. A* **84**, 043804 (2011).
- [35] J. Dalibard, F. Gerbier, G. Juzeliūnas, and P. Öhberg, Colloquium: Artificial gauge potentials for neutral atoms, *Rev. Mod. Phys.* **83**, 1523 (2011).
- [36] K. Fang, Z. Yu, and S. Fan, Photonic Aharonov-Bohm Effect Based on Dynamic Modulation, *Phys. Rev. Lett.* **108**, 153901 (2012).
- [37] K. Fang, Z. Yu, and S. Fan, Realizing effective magnetic field for photons by controlling the phase of dynamic modulation, *Nat. Photon.* **6**, 782 (2012).
- [38] N. A. Estep, D. L. Sounas, J. Soric, and Andrea Alù, Magnetic-free non-reciprocity and isolation based on parametrically modulated coupled-resonator loops, *Nat. Phys.* **10**, 923 (2014).
- [39] V. Peano, C. Brendel, M. Schmidt, and F. Marquardt, Topological Phases of Sound and Light, *Phys. Rev. X* **5**, 031011 (2015).
- [40] M. Schmidt, S. Kessler, V. Peano, O. Painter, and F. Marquardt, Optomechanical creation of magnetic fields for photons on a lattice, *Optica* **2**, 635 (2015).
- [41] K. Fang, J. Luo, A. Metelmann, M. H. Matheny, F. Marquardt, A. A. Clerk, and O. Painter, Generalized non-reciprocity in an optomechanical circuit via synthetic magnetism and reservoir engineering, *Nat. Phys.* **13**, 465 (2017).
- [42] P. Roushan *et al.*, Chiral ground-state currents of interacting photons in a synthetic magnetic field, *Nat. Phys.* **13**, 146 (2017).
- [43] L. Jin and Z. Song, Incident Direction Independent Wave Propagation and Unidirectional Lasing, *Phys. Rev. Lett.* **121**, 073901 (2018).
- [44] X. Guan, Y. Feng, Z.-Y. Xue, G. Chen, and S. Jia, Synthetic gauge field and chiral physics on two-leg superconducting circuits, *Phys. Rev. A* **102**, 032610 (2020).
- [45] A. A. Clerk, Introduction to quantum non-reciprocal interactions: from non-Hermitian Hamiltonians to quantum master equations and quantum feedforward schemes, [arXiv:2201.00894](https://arxiv.org/abs/2201.00894).
- [46] X. Wang, H.-R. Li, and F.-L. Li, Generating synthetic magnetism via Floquet engineering auxiliary qubits in phonon-cavity-based lattice, *New J. Phys.* **22**, 033037 (2020).
- [47] D. F. James and J. Jerke, Effective Hamiltonian theory and its applications in quantum information, *Can. J. Phys.* **85**, 625 (2007).
- [48] D. Cilluffo, A. Carollo, S. Lorenzo, J. A. Gross, G. M. Palma, and F. Ciccarello, Collisional picture of quantum optics with giant emitters, *Phys. Rev. Res.* **2**, 043070 (2007).
- [49] L. Du, Y.-T. Chen, Y. Zhang, and Y. Li, Giant atoms with time-dependent couplings, *Phys. Rev. Res.* **4**, 023198 (2022).
- [50] J. Vidal, R. Mosseri, and B. Douçot, Aharonov-Bohm Cages in Two-Dimensional Structures, *Phys. Rev. Lett.* **81**, 5888 (1998).
- [51] J.-T. Shen and S. Fan, Coherent Single Photon Transport in a One-Dimensional Waveguide Coupled with Superconducting Quantum Bits, *Phys. Rev. Lett.* **95**, 213001 (2005).
- [52] J.-T. Shen and S. Fan, Theory of single-photon transport in a single-mode waveguide. I. Coupling to a cavity containing a two-level atom, *Phys. Rev. A* **79**, 023837 (2009).